Examining the Evidence for Chthonian Planets: Superdense Exposed Exoplanet Cores

by

Haley Bates-Tarasewicz

Submitted to the Department of Earth, Atmospheric and Planetary Sciences

in partial fulfillment of the requirements for the degree of

Bachelor of Science in Earth, Atmospheric and Planetary Sciences

at the

MASSACHUSETTS INSTITUTE OF TECHNOLOGY

June 2019

Author . . . . . Signature redacted . . . . . .

Department of Earth, Atmospheric and Planetary Sciences

May 22, 2019

Certified by. . . . Signature redacted . . . . . .

Benjamin Weiss

Professor

Thesis Supervisor

Accepted by. . . . . Signature redacted . . . . . .

Richard P. Binzel

Chairman, Department Committee on Undergraduate Theses

Examining the Evidence for Chthonian Planets: Superdense Exposed Exoplanet Cores

by

Haley Bates-Tarasewicz

Submitted to the Department of Earth, Atmospheric and Planetary Sciences
on May 22, 2019, in partial fulfillment of the
requirements for the degree of
Bachelor of Science in Earth, Atmospheric and Planetary Sciences

Abstract

Planetary cores are of interest because they provide insight into the internal dynamics and composition of planets. By using mass-radius relationship compositional analysis, this work originally set out to look for evidence of exoplanet exposed iron cores; it stumbled, however, upon potential superdense core candidates (or "Chthonian" cores). We identify 19 potential superdense core candidates, and compare them to the Fossilized Core Theory and the Giant Impact Theory of formation. Additionally, while there are 19 superdense core candidates, they represent only 11 solar systems. We find that both theories plausibly describe the formation of these superdense candidates, and note that all candidates have very typical stars similar to our own sun. Until the mass measurements of the candidates are better constrained, further conclusions cannot be drawn, however, this new type of planet could help inform planetary formation, evolution, and interior dynamic models.

Thesis Supervisor: Benjamin Weiss Title: Professor

1. INTRODUCTION

The discovery and confirmation of thousands of exoplanets in the past few decades has provided the opportunity to examine the edge cases and extremes of planetary evolution, putting our own solar system in a context of increasing complexity.

While the search continues for a solar system analogue, what's still intriguing is when types of planets are found that are not present in our own solar system — large planets that bridge the gap between planet and star (Bouchy *et al.*, 2011), small planets the size of the Earth's moon (Sinukoff *et al.*, 2013), low-density planets thought to have tails like comets (Croll *et al.*, 2017), the sheer number of Hot Jupiters existing so close to their host stars (Currie, 2009). Planets have been discovered that appear to be actively losing their atmospheres (Catlin and Zahnle, 2009), or that may have survived being engulfed by their host stars (Charpinet, *et al.*, 2011). Entire families of planets that are outside of our expectations in some way (such as Lissauer *et al.*, 2013) — all of these variations provide context for the typicality of our own solar system. As new planets are discovered, our understanding of the mechanisms governing planetary dynamics are iterated and improved upon, and the methods used to understand unexpected exoplanets have proliferated.

In addition to allowing new views of planetary extremes, a growing pool of exoplanets also means we are able to study planets in all states of their evolution — planets still in their protoplanetary disks, or planets substantially older than our own solar system (Anglada-Escude, *et al.*, 2014) — which help to understand how our solar system came to be and what we can expect it to turn into eventually.

As more exotic exoplanets are discovered, an understanding of their interior composition and dynamics becomes more and more valuable. The cores of planets are of particular interest because they are indicative of the planetary formation process and evidence of past solar system conditions. Even within our own solar system, planetary missions recently have been preoccupied with cores: the Psyche mission, which in 2020 will visit an M-type asteroid known as 16-Psyche, thought to be the exposed remnant of a differentiated protoplanetary core (Elkins-Tanton *et al.*, 2014); the InSight mission, which is currently studying the core of Mars looking for geologic activity and recently detected evidence of a Marsquake (Brown and Johnson, 2019); and Juno, a Jupiter probe which is expected to provide valuable information on the characteristics of Jupiter's core in the upcoming years (Cheng *et al.*, 2008).

Exposed cores are particularly interesting because they allow near direct observation of the interior of a planet. While our own solar system is thought to contain examples of exposed planetary cores such as 16-Psyche and Mercury (Elkins-Tanton *et al.*, 2014), examples of cores in other solar systems would allow for a more general understanding of the role solar system conditions play in planetary

evolution. Broadly speaking, there are thought to be two ways in which planets can lose their outer mass, leaving their cores exposed.

The first mechanism is through powerful impacts in the early solar system (Kendall and Melosh, 2016). These impacts are thought to have been quite common, and under some planetary formation mechanisms are thought to have been necessary for planet formation. In extreme cases, the energy of the impact could have stripped one or both bodies of their outer layers, leaving only the dense, differentiated metallic cores (Kendall and Melosh, 2016; Righter and O'Brein, 2010). This process is best understood for terrestrial planets, though could potentially occur with gas giants.

The second mechanism is through extreme thermal environments. Terrestrial planets are thought to be able lose their mantles (Bonomo *et al.,* 2019) through photoevaporation and vaporization, while gas giants are thought to undergo hydrodynamic escape of their envelopes (Catling and Zahnle, 2009; Ehrenreich *et al.,* 2015; Herbrard *et al.,* 2003; Moquet *et al.,* 2014).

This work originally set out to identify iron-rich cores of terrestrial planets; it stumbled, however, upon potential superdense core candidates. Superdense planets have not been studied in depth in the past and are not predicted by most planetary formation or evolution mechanisms (Moquet *et al.,* 2014).

In this work, we examine 19 superdense planetary core candidates, and compare them to two potential formation mechanisms: the Fossilized Core Theory (Moquet *et al.,* 2014), and the Giant Impact Theory (Bonomo *et al.,* 2019). We find that while there are 19 superdense core candidates, they represent only 11 individual solar systems. Solar system clustering of exotic exoplanets could imply a stellar dependent evolution mechanism, so the stellar properties of the identified systems are examined for patterns.

While the data are too unconstrained to make definitive conclusions, we find that both mechanisms are plausible explanations for the observed states. We also find that all of the superdense core candidates orbit main-sequence, relatively cool or G-type stars.

Cores of this type are occasionally called "Chthonian", as "Chthonian" means concerning, belonging to, or inhabiting the underworld. It implies the ability to view what is typically hidden. To further understand the potential for Chthonian cores to exist, the masses of all of the candidates examined here must be further constrained. Additionally, more sophisticated relaxation models and giant impact stripping models must be further developed.

2. METHODS

2.1 Mass-Radius Relationship and Equation of State

Originally, the goal of this work was to look for evidence of exposed exoplanet cores in general, following a composition-focused approach. Similar to other studies looking to understand the internal structure and compositions of exoplanets and other celestial bodies, this study used mass-radius (M-R) relationships as a classification tool (Leger *et al.,* 2004; Valencia *et al.,* 2006; Valencia *et al.,* 2007; Zapolsky and Salpeter, 1969).

The composition of a planet can be estimated by comparing its measured radii to that of a hypothetical sphere of a proposed composition of the same mass (Seager *et al.*, 2007; Swift *et al.,* 2012; Zeng *et al.,* 2016, Zeng *et al.,* 2017) . However, this form of estimating bulk composition is highly degenerate; by mass-radius data alone, there is no way, for example, to reliably differentiate a planet made entirely out of water from one made of iron with a thick hydrogen atmosphere (Seager *et al.*, 2007). In these cases, assumptions about planetary formation mechanisms, elemental abundance, or planetary family need to be made to propose a given composition (Grasset *et al.*, 2009).

However, making assumptions based on typical compositions or classifications may have the consequence of overlooking atypical possibilities, such as when the bodies have unusual thermal or compressive states. Because edge cases and extremes are so useful for understanding the full scope of planetary formation mechanisms, it is worthwhile to thoroughly examine any potential outliers, as was done in this study.

This work aimed to identify examples of the dense, exposed cores of differentiated terrestrial bodies, which are thought to be made mostly of iron (Ehrenreich *et al.,* 2015; Elkins-Tanton *et al.,* 2014; Kendall and Melosh, 2016; Mocquet *et al.,* 2014). Candidates were therefore compared to a M-R relationship indicative of a homogeneous sphere of iron.

In many cases, M-R relationships are found from specific equations of state (EOS) derived from empirical data (Seager *et al.,* 2007). However, Seager *et al.*, (2007) found that the EOSs for many solid materials share a similar form, and proposed a generic modified polytropic EOS applicable to a variety of materials, accounting for the low compressibility of solids and liquids at low pressures. From the generic EOS, a generic M-R relationship was found. Applying Seager's generic M-R relationship to iron, the exact M-R relationship used in this study was:

$$log_{10}(R_s) = k_1 + \tfrac{1}{3} log_{10}(M_s) - k_2 M_s^{k_3} \quad (1)$$

where

$$R_s = \frac{R}{R_1}$$

$$M_s = \frac{M}{M_1}$$

where the constants R_s, M_s, k_1, k_2, and k_3 vary depending on the material. For iron, these values are shown in Table 1.

Table 1: Constants for generic mass radius relationship as applied to iron

Constant:	R_1	M_1	k_1	k_2	k_3
Value:	$2.25R_{Earth}$	$5.8M_{Earth}$	-0.20945	0.0804	0.394

This approach is not without issues. The M-R relationship given above is only valid for planets of up to about $20M_{Earth}$, and while it approximates zero-temperature and 300K temperature EOSs well, it is unknown how it performs with hotter temperatures. However, because the planets examined in this work have relatively large uncertainties, it is not expected that the small errors in the iron M-R relationship due to higher temperatures etc. would have a significant effect on the analysis.

2.2 Initial Data

The Extrasolar Planets Encyclopaedia (exoplanet.eu) provided the initial data for this study. At the time of this writing, exoplanet.eu had data for 3715 confirmed exoplanets. Published values for mass and/or radius were missing for 2547, and so those candidates were discarded as composition analysis requires an understanding of both mass and radius (Mocquet *et al.*, 2014). Finally, though the iron M-R relationship presented above is only accurate to approximately $20M_{Earth}$, planets up to $100M_{Earth}$ were considered for context, leaving 236 analyzable candidates. Figure 1 presents the preliminary mass-radius data along with the iron M-R relationship.

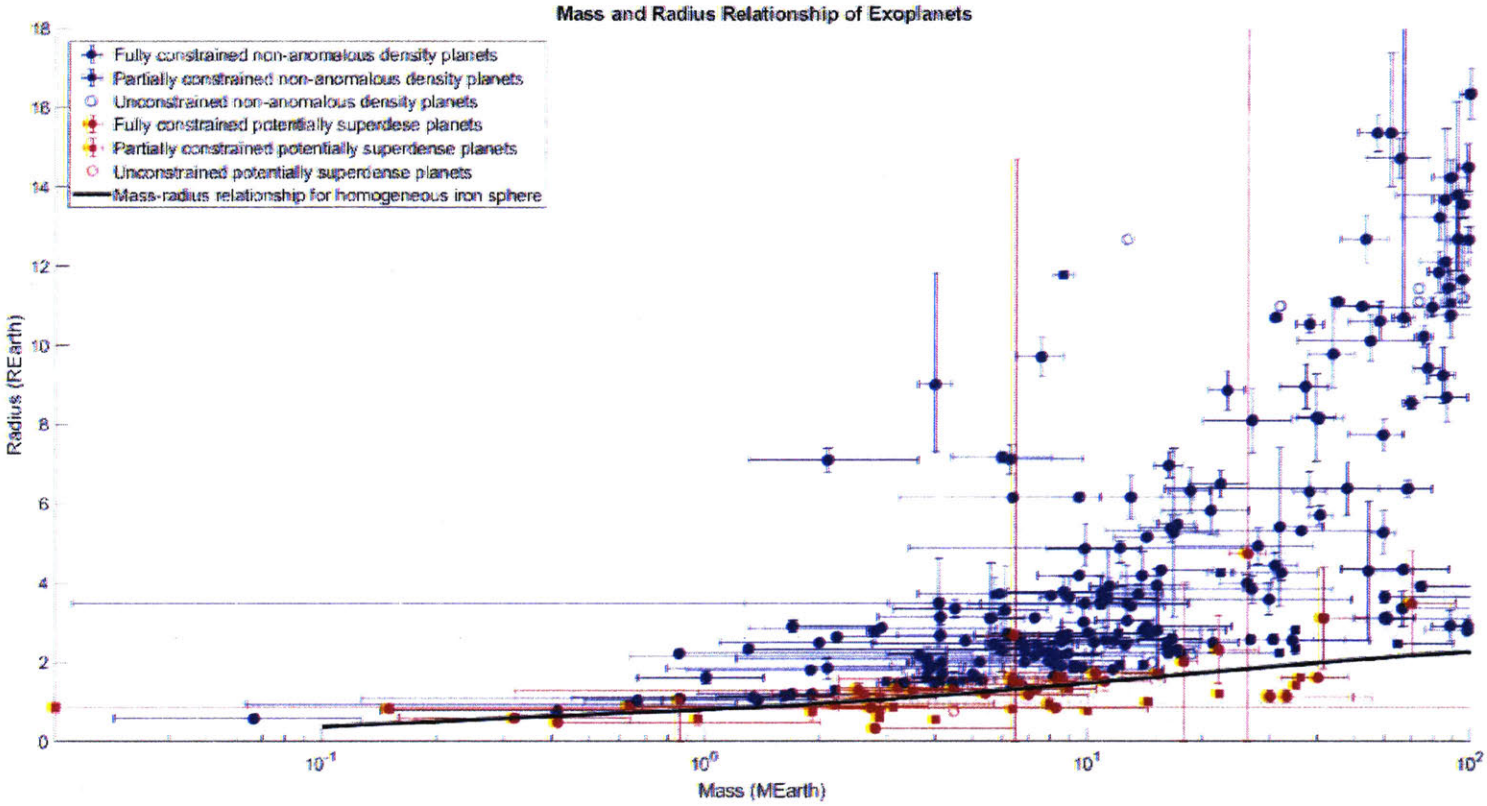

Fig 1: Preliminary identification of superdense core candidates

Shown is the mass and radius (scaled by the Earth's mass and radius) of 236 viable planets less than $100M_{Earth}$, highlighting the division between planets with radii larger than an iron sphere of the same mass (blue) and those with radii potentially smaller than that of an iron sphere of the same mass (red). This division corresponds to planets that are less dense than iron and those that are potentially more dense than iron, respectively. Data retrieved from exoplanet.eu.

This work initially set out to attempt to identify planets with a composition very close to that of iron; however, more intriguing were those planets that lie significantly below the iron M-R line. Iron is the densest cosmically abundant element (Ehrenreich *et al.*, 2015; Elkins-Tanton *et al.*, 2014; Kendall and Melosh, 2016; Mocquet *et al.*, 2014), and there are no widely accepted planetary formation theories that would allow for significant amounts of materials denser than iron to be present. Barring incorrectly reported values or errors in data analysis by initial publishers, the superdense candidates imply an unusual history.

Focusing on the superdense candidates, all points with uncertainty regions above the iron M-R relationship were additionally discarded, leaving 24 preliminary superdense core candidates (Figure 2).

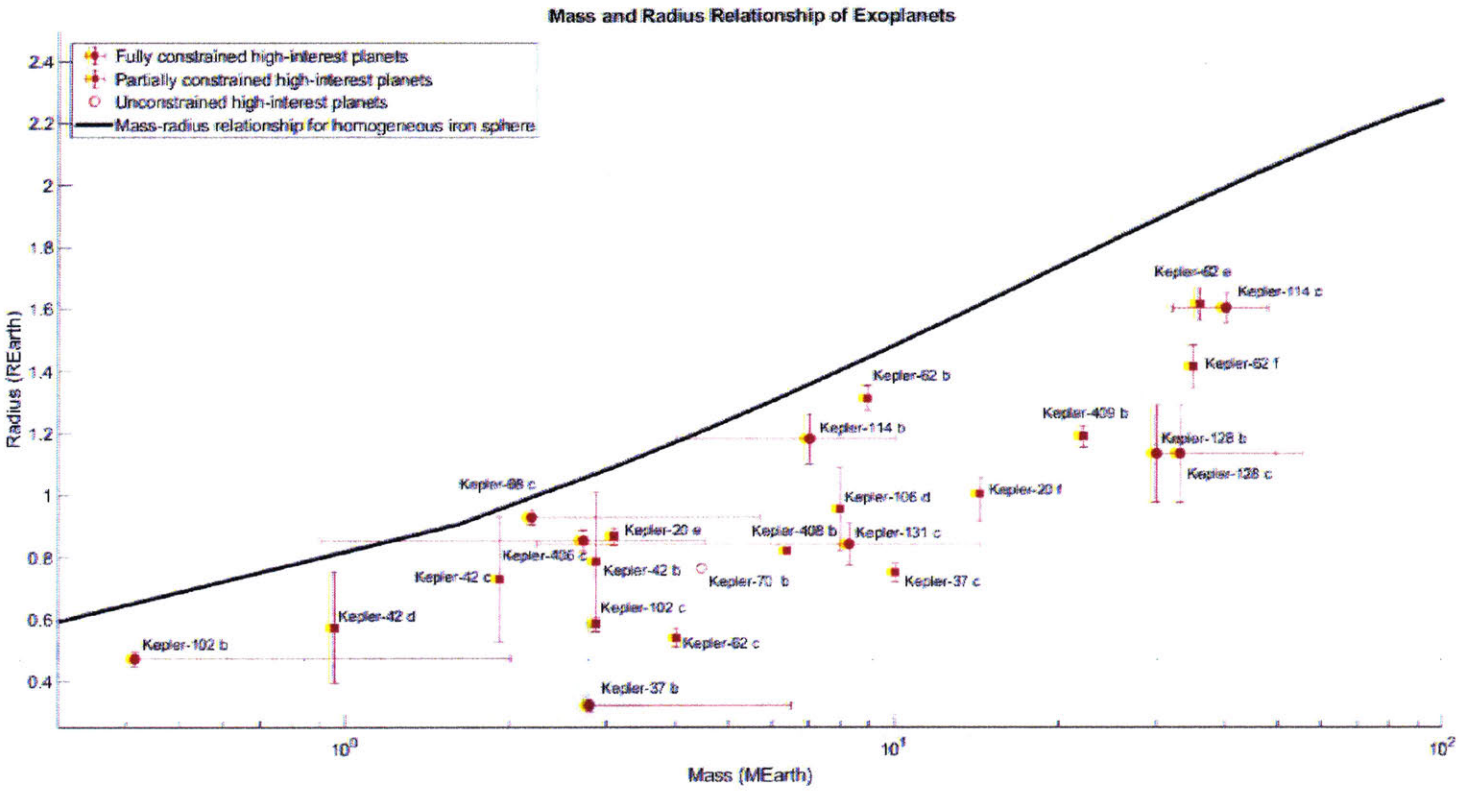

Fig 2. Focused identification of superdense core candidates

Mass and radius (scaled by the Earth's mass and radius) for high-interest potentially superdense candidates less than $100M_{Earth}$. Only points that were statistically likely (based on published uncertainty) to lie beneath the pure iron case (shown in black) were included. The names of the planets are adjacent to their respective points. Data retrieved from exoplanet.eu.

This work is not the only work that has identified unexpectedly dense exoplanets. In 2006, Fortney *et al.* identified a metal rich transiting exoplanet. In 2017, Luque *et al.* detected and characterized an ultra-dense sub-Neptune planet. Also in 2017, Guenther *et al.* studied a system with one metal-rich planet amongst other lower-density planets. In 2018, Santerne *et al.* found an Earth-sized exoplanet with a Mercury-like dense composition. Just this year (2019), Price and Rogers investigated an iron-rich planets orbiting close to their host stars. However, none but Moquet *et al.* (2014) have examined planets with bulk density significantly higher than that of iron.

2.3 Proposed Mechanism 1: Fossilized Core Theory

Mocquet *et al.* (2014) is an important work with which to compare this study to, as they also investigated superdense planets of this nature, identifying ten potentially superdense candidates and

focusing analysis on three examples (Kepler-52 b, Kepler-52 c and Kepler-57 b; see Figure 3). While all of Moquet's other candidates are considered in this analysis, it is notable that these three are excluded because while Mocquet *et al.* also used exoplanet.eu as a data source, the entries for the mass and radius data for these high-interest candidates were updated after Mocquet *et al.* was published.

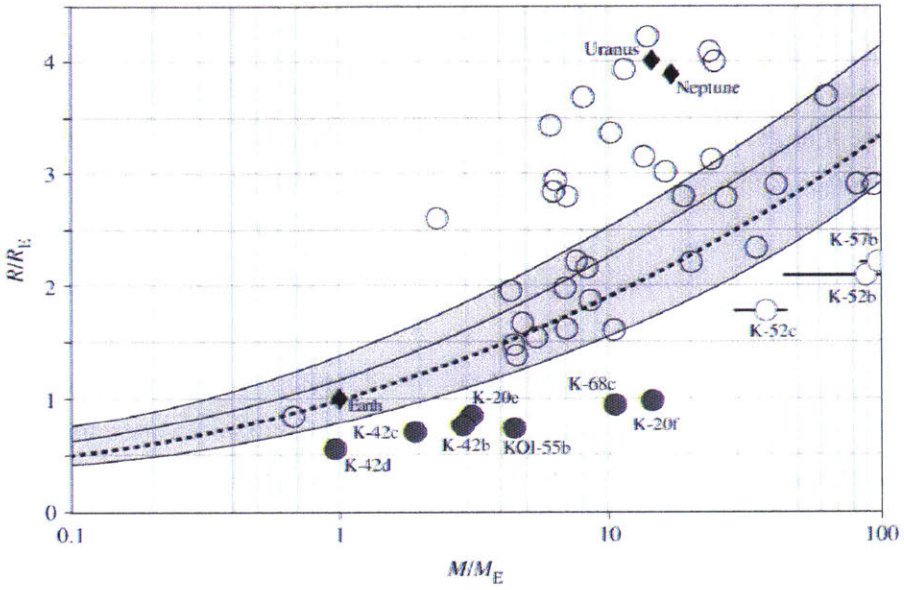

Fig 3. Mass and radius for Mocquet et al.'s 10 superdense exoplanet core candidates

The four curves are, with increasing density from the top of the figure to the bottom, pure H_2O, 'Ocean Planets' (50% H_2O, 50% Silicates), 'Earth-Like Planets' (dashed and bold), and pure iron. The white circles represent planets with independent M-R estimates, while the grey circles represent planets for which the mass is still badly constrained and model-dependent. In the latter case, the point is represented by the densest case proposed in the literature. Figure reprinted from Mocquet *et al.* (2014).

Mocquet *et al.* was submitted in 2013, and published in April of 2014. The entries for Kepler-52 b, Kepler-52 c, and Kepler-57 b were last updated in May of 2014, October of 2018, and June of 2017 respectively. In Mocquet's study, exoplanet.eu cited analytic mass limits derived from transit timing variation (TTV) data. However, since the publishing of Mocquet *et al.* (2014), the exoplanet.eu masses were updated to reflect the mass limits determined from orbital stability considerations, which are notably larger than those determined analytically. As a result, the published mass limits for the three candidates vary by on the order of $1000M_{Earth}$ between this study (Steffen *et al.* 2013) and Mocquet's. Because this study did not consider planets with an exoplanet.eu published mass of more than $100M_{Earth}$, the three high-interest candidates examined in Mocquet *et al.* (2014) were not considered here.

Mocquet *et al.* (2014) proposed a mechanism for the formation and evolution of superdense planets known as the "Fossilized Core Theory," evaluating their ten superdense candidates against the

mechanism. Of the candidates found in this study, 16 have had new data reported or updated after the publication of Mocquet *et al.* (2014) As a result, with the exception of KOI-55 and the Kepler-42 planets, all of the candidates marked in grey in Figure 3 have since been updated with experimentally determined mass estimates, as discussed later in Section 3.

The Fossilized Core Theory proposed by Mocquet *et al.* (2014) theorizes that the observed superdense planets are actually the stripped cores of gas or ice giants. Generally, this process is thought to happen when a gas or ice giant migrates close enough to its host star to undergo hydrodynamic escape, stripping the planet of its gas or ice envelope and leaving behind the compressed chthonian "fossilized" core. This process requires four stages: compression, migration, thermal escape, and decompression (Moquet *et al.* 2014).

Compression:

The Fossilized Core Theory suggests that the observed superdense planets formed as gas or ice giants. Giant planets are thought to have notably high central pressures (Saumon and Guillot, 2004), plausibly enough to compress their rock and iron cores to near the observed densities of the anomalous superdense planets. Though the core densities of the gas and ice giants in our own solar system are poorly understood, some models predict Jupiter's core to be ~25g/cm ^{3} (Wolf and Wood, 2007), which is heavier than iron by nearly a factor of four. It is plausible for the cores of gas or ice giants to have cores with similar densities to the superdense candidates.

Migration

In order for the superdense cores to be exposed, it is thought that the gas or ice giant must be in a thermal environment such that the envelope escapes, *i.e.*, it must be close enough to its host star to undergo hydrodynamic escape.

Planetary migration has been studied studied in depth (Beague and Nesvory, 2012; Masset and Papaloizou, 2003; Nelson *et al.*, 2014; Wu and Lithwick, 2011) since the discovery of so-called 'Hot Jupiters', or giant planets that are far closer to their host stars than expected by widespread planetary formation mechanisms. In-situ formation of Hot Jupiters is incompatible with nearly every existing planetary formation model, so many plausible migration methods have been proposed to explain their observed positions (Beague and Nesvory, 2012; Masset and Papaloizou, 2003; Nelson *et al.*, 2014; Wu and Lithwick, 2011).

Thermal Escape

Many models exist to describe the atmospheric loss of Hot Jupiters (Catling and Zahnle, 2009; Hebrard *et al.* 2003; Tian *et al.* 2005). The thermal escape method of the eroding planetary envelope proposed by the Fossilized Core Theory may be dominated by one of three processes depending on the spatial, thermal, and compositional variations in the star, orbit, and planetary atmosphere. The three processes are either energy-limited escape, diffusion-limited escape or escape through blow-off (Mocquet *et al.*, 2014; Tian *et al.*, 2008) . Valencia *et al.* (2010) applied the extreme case of energy limited escape (where the atmospheric loss is proportional to the corrected ratio between the flux of the stellar ultraviolet radiation and the gravitational potential of the planet; see Yelle *et al.* 2008) to CoRot-7 b and found an atmospheric loss rate of 108 kg s-1. This is supported by the 102 - 109 kg s-1 range hypothesized by Lecavelier des Etangs (2007). Valencia *et al.* (2010) proposed that a hydrogen-helium atmosphere would escape in 1Myr, while a water atmosphere would escape in closer to 1Gyr. The relatively short timescales of atmospheric loss are particularly important to keep in mind when considering the decompression rates of the unloaded core.

Decompression

Once the gas envelope has eroded, the Fossilized Core Theory suggests that the cores are left to slowly decompress back to traditional expected densities, and suggests they would be nearly indistinguishable from terrestrial planets (Mocquet *et al.*, 2014). In order to detect them, observations would need to be taken during the decompression stage. If decompression does not take significantly longer to achieve than the hydrothermal escape of the gas or ice envelopes, it is unlikely that the observed planets formed by this mechanism.

Mocquet *et al.* (2014) calculated the time-varying evolution of the volumetric strain experienced by the planetary core during and after atmospheric escape, assuming stellar abundances of elements. The solid core rheological response was described through a viscoelastic Maxwell rheology they defined by three parameters: incompressibility derived from EOS, the viscosity, and the Poisson ratio.

Their results imply that for extremely high pressures, the unloading stress on the core can drastically affect the temporal evolution of the strain, in some situations even leading to a loss of cohesion of the planet if the atmospheric loss rate is significantly high (Mocquet *et al.* 2014).

Their results suggest that for large planetary cores, the relaxation timescales may be several billions of years after atmospheric loss, making it plausible that the naked cores could be observed from Earth today, though their results do not take into account the rheological stratification of the planet, which could lead to further brittle deformations in the uppermost high-viscosity layers of the planet. If brittle deformations occur, the relaxation rates will not slowly, smoothly decompress as discussed here, but

instead crack and splinter. It is not well understood how broken, cracked planets could be detected or what they would look like if observed (Mocquet *et al.*, 2014).

The Fossilized Core Theory was examined in Section 4.1 below as a potential formation mechanism for the additional planets identified in this study.

2.4 Proposed Mechanism 2: Giant Impact Theory

A similarly important work to examine in relation to this study is Bonomo *et al.* (2019), where they were able to explain the unexpectedly high density of Kepler-107 c via giant impacts. The Kepler-107 c system is intriguing, as the two inner planets have nearly the same radii (1.5-1.6$R_{\oplus}$), however Kepler-107 c is nearly twice as dense (12g/cm ^{3}) as Kepler-107 b (5.3g/cm ^{3}).

Kepler-107c appeared in the preliminary M-R plot examined in this study; however, it was discarded as the region bounded by its error in mass and radius did not lay entirely or nearly entirely under the M-R iron relationship. The planets considered by Bonomo *et al.* (2019) (including Kepler-107 b and Kepler-107 c) do however have better constrained masses than those examined in this study (Section 3) with bulk densities measured to at least 33% precision.

Bonomo *et al.* (2019) proposed that the disparity in densities between the two innermost Kepler-107 planets could be due to a giant mantle-stripping impact that removed enough of the silicate mantle of Kepler-107c to increase its mean density. Under most planetary formation mechanisms, it is expected that if a disparity in density is to occur, the innermost planet would be the densest due to photophoresis and disk aerodynamic fractionation causing a silicate-poor inner disk region (Bonomo *et al.*, 2019). Similarly, under most mantle stripping mechanisms from thermal or radiation sources, it is likewise expected that the innermost planet be denser if a disparity is to exist, as innermost planets are subject to the most energetic thermal or radiative environments (Bonomo *et al.*, 2019). The fact that Kepler-107 c was found to have a higher density than its innermore companion despite these expectations is intriguing.

Figure 4 shows the M-R relationship for the considered planets against a variety of compositional theoretical M-R relationships including the maximally collisionally stripped case. It also uses color to demonstrate the hottest planets are not the densest in this case.

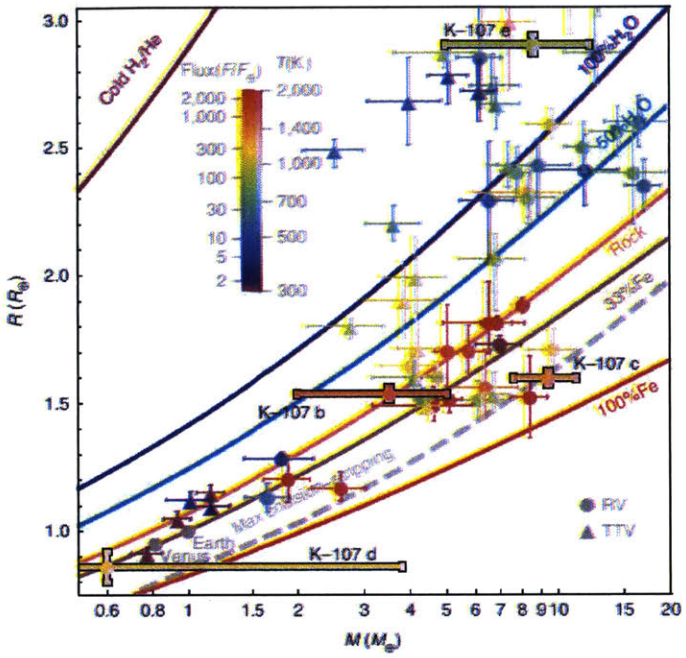

Fig 4. Mass and radius for Bonomo et al.'s planets under 3R⊕

The figure includes only planets with bulk densities measured to better than 33% precision through transit timing variation (triangles) or radial velocity (circles). The shown error bars represent 1σ confidence intervals. The planet marker colors represent planet equilibrium temperature assuming an Earth-like albedo. Notice Kepler-107b is more irradiated, yet less dense than Kepler-107c. The solid lines represent theoretical M-R relationships for various compositions, while the grey dashed line represents the theoretical M-R relationship for the max collision stripping case. Figure reprinted from Bonomo *et al.* (2019).

Generally, the giant impact theory is one of the better ways to explain outer planets with significantly higher densities than those closer in, and fits the case of Kepler-107 c consistently (Bonomo *et al.* 2019). Kepler-107 c falls nicely on the expected curve for max collisional stripping in Figure 4 above, which already suggests it may be in accordance with the giant impact theory. Further, for low-eccentricity systems like Kepler-107, the possibility of a denser planet forming close to the star and then migrating outwards beyond its companions (the other proposed formation mechanism) is unlikely, as the orbit-crossing event would likely need to happen before the dispersal of the protoplanetary disk to achieve dampened eccentricities (Bonomo *et al.* 2019). With the relatively large mass of Kepler-107 c, it is also unlikely that the planet would be able to migrate before the protoplanetary disk to dissipate, making it most likely to have been formed from the giant impact method than other theories investigated (Bonomo *et al.* 2019).

Marcus *et al.* (2010) developed the model for the max collisional stripping M-R relationship used in Figure 4 to assess the Kepler-107 system, and is shown on its own in Figure 5. The goal of their model

was to find the smallest possible remnant after impact. They assumed differentiated rocky super Earths composed of only iron and silicates would yield the minimum pre-impact radius for a given mass, and so would also yield the minimum post-impact radius for a given mass. They posit that the only way to significantly increase the mean density is to remove the silicate mantle while maintaining the iron core, and suggest that giant impacts are the most efficient way to do so (Marcus *et al.*, 2010).

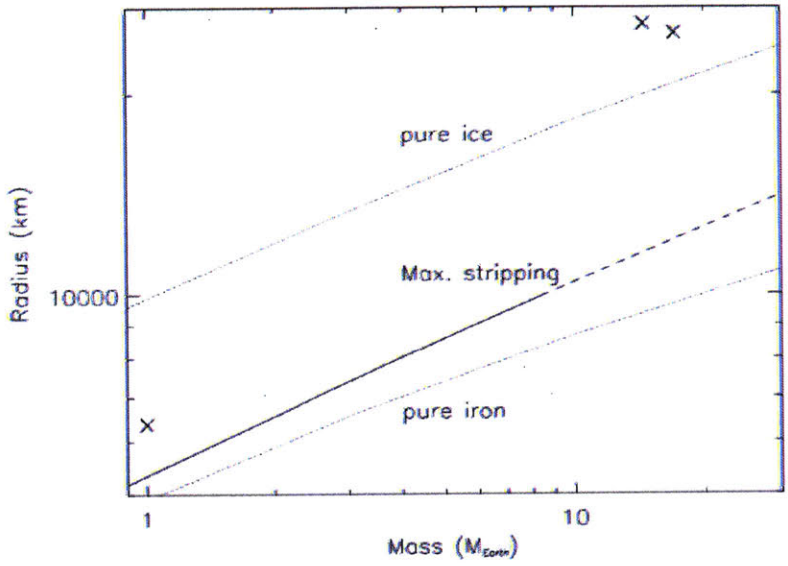

Fig 5. Marcus et al.'s max collisional stripping relationship

The dotted lines represent the hypothetical M-R relationships for pure water ice and pure iron. The solid line is the determined M-R relationship for the maximum mantle stripping due to impacts, corresponding to an 80km/s impact with equal projectile target masses. The dashed portion of the Max Stripping M-R relationship corresponds to cases for target masses greater than $15M_{\oplus}$. The 'x' symbols are the masses and radii of Earth, Uranus, and Neptune. Figure reprinted from Marcus *et al.* (2010).

To determine their max collisional stripping M-R relationship, Marcus *et al.* (2010) first start off with a three assumptions. First is that all super-Earth sized bodies are differentiated, which is not restrictive as all large planets and satellites in our own solar system are thought to be differentiated. The second is the assumption of solar system abundances. They state that the most effective collisions for increasing the overall bulk density are most likely equal mass, head on encounters where both bodies are made primarily of iron and silicates without significant fractions of volatiles or gasses (Marcus *et al.* 2010). Applying solar system abundances, they find a max iron core fraction Si/Fe of ~0.6, and use it as a proxy for mantle-to-core mass fraction (Marcus *et al.* 2010). Lastly, the M-R relationship for max collisional stripping assumes all of the mass is stripped in a single, late giant impact (though A. Chau *et*

al. (2018) examines multiple impact cases), and that none of the lost mass is re-accreted afterwards (Marcus *et al.*, 2010).

Super Earths are thought to form in the mass range 1-15$M_{\oplus}$, after which runaway gas accretion is thought to occur and they become gas giants. As such, this max collisional stripping M-R relationship is only understood for rocky super Earths (Marcus *et al.*, 2010).

Inamdar and Schlichting (2016) showed that giant impacts between similarly sized planets with large envelopes can reasonably reduce the envelope-to-core-mass ratio by factors of two, which leads to a mean density increase by factors of two to three, though they did not publish a M-R relationship as Marcus *et al.* (2010) did.

The giant impact method was examined in Section 4.2 as a potential formation mechanism for the planets in this study.

2.5 Stellar Properties

These 24 proposed candidates represent only fourteen unique solar systems, meaning that several candidates share the same host star. The tendency for there to be multiple Chthonian cores in the same solar system could imply that the long-term planetary evolution of these bodies is in some way dependent on stellar type.

The spectral type, mass, and radius of the host stars were also examined in an attempt to look for other underlying patterns in Section 4.3.

3. RESULTS

The mass measurements from exoplanet.eu used to create the preliminary M-R relationship of superdense core candidates in Figures 1 and 2 were suspiciously constrained. As a general rule, mass measurements are noisier than radius measurements, and the fact that many candidates had masses with no published error at all prompted a reevaluation before moving forward with the analysis.

After examining the most recent mass and radius publications for each superdense candidate, we found that exoplanet.eu was fairly inconsistent with publishing the mass values that the original authors were most confident in. Like the case with Moquet *et al.* (2014) in Section 2.3, if a paper published multiple mass estimates from multiple methods, the database occasionally did not report the 'best' value. Likewise, the database was unreliable at differentiating when a measurement was an upper bound to the mass and when the mass had no published uncertainty. The latter fact was responsible for the unconstrained mass measurements in Figures 1 and 2. The updated masses and true published error for each of the superdense candidates is found in Table 2 below.

In the verification of the exoplanet.eu data, we also found that some of the candidates had had more recent publications refining the mass or radius data that exoplanet.eu did not reflect. Five of the planets (Kepler-114 b, Kepler-114 c, Kepler-128 b, Kepler-128 c, and Kepler-70 b) that had previously been identified as superdense had more constrained mass data published from TTV analysis or had data misreported in the exoplanet.eu database, and are no longer included in this study, leaving 19 total superdense candidates.

While there are 19 chthonian core candidates, only 11 solar systems are represented. Because more than one superdense planet per solar system may imply a stellar component to their formation or evolution, the stellar parameters were also retrieved. The data used for the remainder of this work are located in Table 2 below.

Table 2: Planetary and stellar parameters used in this study

Planet Name	Planet Mass (M_{Jup})	Planet Radius (R_{Jup})	Period (days)	Stellar Mass ($M_\odot$)	Stellar Radius ($R_\odot$)	T_{eff} (K)	Semimajor Axis (AU)[1]	Stellar Class	References
Kepler-20 *e**	< 0.0097	$0.0772^{+0.0023}_{-0.0025}$	$6.0985^{+6.08E-06}_{-1.35E-05}$	$0.912^{+0.035}_{-0.035}$	$0.944^{+0.095}_{-0.095}$	$5466.0^{+93.0}_{-93.0}$	0.0633	G5V C	Fressin *et al.* (2012) Frasca *et al.* (2016)
Kepler-2 *f**	< 0.045	$0.0895^{+0.0045}_{-0.0079}$	$19.578^{+9.04E-05}_{-0.000123}$	$0.912^{+0.035}_{-0.035}$	$0.944^{+0.095}_{-0.095}$	$5466.0^{+93.0}_{-93.0}$	0.138	G5V C	Fressin *et al.* (2012) Frasca *et al.* (2016)
Kepler-37 *b**†	< 0.0315	$0.0285^{+0.0018}_{-0.0018}$	$13.367^{+5.80E-05}_{-8.50E-05}$	$0.803^{+0.068}_{-0.068}$	$0.77^{+0.026}_{-0.026}$	$5417.0^{+75.0}_{-75.0}$	0.102	K0	Marcy *et al.* (2014)
Kepler-37 *c**†	< 0.0378	$0.0669^{+0.00268}_{-0.00268}$	$21.302^{+4.60E-05}_{-4.60E-05}$	$0.803^{+0.068}_{-0.068}$	$0.77^{+0.026}_{-0.026}$	$5417.0^{+75.0}_{-75.0}$	0.14	K0	Marcy *et al.* (2014)
Kepler-42 *b*‡	< 0.009	$0.07^{+0.02}_{-0.02}$	$1.214^{+4.60E-06}_{-4.60E-06}$	$0.13^{+0.05}_{-0.05}$	$0.17^{+0.05}_{-0.05}$	$3068.0^{+174.0}_{-174.0}$	0.0113	M4V C	Muirhead *et al.* (2012a) Muirhead *et al.* (2012b)
Kepler-42 *c*‡	< 0.006	$0.065^{+0.018}_{-0.018}$	$0.453^{+9.70E-07}_{-9.70E-07}$	$0.13^{+0.05}_{-0.05}$	$0.17^{+0.05}_{-0.05}$	$3068.0^{+174.0}_{-174.0}$	0.00585	M4V C	Muirhead *et al.* (2012a) Muirhead *et al.* (2012b)
Kepler-42 *d*‡	< 0.003	$0.051^{+0.016}_{-0.016}$	$1.856^{+1.40E-05}_{-1.40E-05}$	$0.13^{+0.05}_{-0.05}$	$0.17^{+0.05}_{-0.05}$	$3068.0^{+174.0}_{-174.0}$	0.015	M4V C	Muirhead *et al.* (2012a) Muirhead *et al.* (2012b)
Kepler-62 *b**†	< 0.028	$0.117^{+0.0036}_{-0.0036}$	$5.7149^{+9.00E-06}_{-9.00E-06}$	$0.69^{+0.02}_{-0.02}$	$0.63^{+0.02}_{-0.02}$	$4925^{+70.0}_{-70.0}$	0.0553	G5 D	Borucki et al (2013) Frasca *et al.* (2016)
Kepler-62 *c**	< 0.0126	$0.048^{+0.0027}_{-0.0027}$	$12.442^{+0.0001}_{-0.0001}$	$0.69^{+0.02}_{-0.02}$	$0.63^{+0.02}_{-0.02}$	$4925^{+70.0}_{-70.0}$	0.0928	G5 D	Borucki et al (2013) Frasca *et al.* (2016)
Kepler-62 *e**	< 0.113	$0.144^{+0.0045}_{-0.0045}$	$122.387^{+0.0008}_{-0.0008}$	$0.69^{+0.02}_{-0.02}$	$0.63^{+0.02}_{-0.02}$	$4925^{+70.0}_{-70.0}$	0.426	G5 D	Borucki et al (2013) Frasca *et al.* (2016)
Kepler-62 *f**	< 0.11	$0.126^{+0.0063}_{-0.0063}$	$267.291^{+0.005}_{-0.005}$	$0.69^{+0.02}_{-0.02}$	$0.63^{+0.02}_{-0.02}$	$4925^{+70.0}_{-70.0}$	0.718	G5 D	Borucki et al (2013) Frasca *et al.* (2016)
Kepler-68 *c**†	< 0.0227	$0.0827^{+0.0022}_{-0.0022}$	$9.605^{+4.50E-05}_{-4.50E-05}$	$1.079^{+1.079}_{-1.079}$	$1.24^{+0.02}_{-0.02}$	$5793^{+74.0}_{-74.0}$	0.0907	G2	Marcy *et al.* (2014)
Kepler-102 *b**	< 0.0135	$0.042^{+0.002}_{-0.002}$	5.287	$0.81^{+0.04}_{-0.09}$	$0.74^{+0.02}_{-0.02}$	4903^{+74}_{-74}	0.0554	K3V C	Marcy *et al.* (2014) Frasca *et al.* (2016)
Kepler-102 *c**	< 0.00944	$0.052^{+0.002}_{-0.002}$	7.0714	$0.81^{+0.04}_{-0.09}$	$0.74^{+0.02}_{-0.02}$	4903^{+74}_{-74}	0.0672	K3V C	Marcy *et al.* (2014) Frasca *et al.* (2016)
Kepler-106 *d**†	< 0.0255	$0.085^{+0.012}_{-0.012}$	23.980	$1^{+0.06}_{-0.06}$	$1.04^{+0.17}_{-0.17}$	5858^{+114}_{-114}	0.163	G2	Marcy *et al.* (2014)
Kepler-131 *c**	< 0.0629	$0.075^{+0.006}_{-0.006}$	25.516	$1.02^{+0.06}_{-0.06}$	$1.03^{+0.10}_{-0.10}$	5685^{+74}_{-74}	0.171	G2V C	Marcy *et al.* (2014) Frasca *et al.* (2016)
Kepler-406 *c**	< 0.0189	$0.076^{+0.003}_{-0.003}$	4.623	$1.07^{+0.06}_{-0.06}$	$1.07^{+0.02}_{-0.02}$	5538^{+75}_{-75}	0.0555	G5IV C	Marcy *et al.* (2014) Frasca *et al.* (2016)
Kepler-408 *b*‡	< 0.0157	$0.073^{+0.0003}_{-0.0003}$	2.565	$1.08^{+0.07}_{-0.07}$	$1.23^{+0.03}_{-0.03}$	6104^{+74}_{-74}	0.0376	F8V C	Marcy *et al.* (2014) Molenda-Zakowicz *et al.* (2013)
Kepler-409 *b**	< 0.0692	$0.106^{+0.003}_{-0.003}$	68.958	$0.92^{+0.06}_{-0.06}$	$0.89^{+0.02}_{-0.02}$	5460^{+75}_{-75}	0.32	K0V C	Marcy *et al.* (2014) Molenda-Zakowicz *et al.* (2013)

[1] Calculated from period assuming circular orbit.

* Planetary masses were only able to be given a 2σ upper bound from RV analysis.

† Stellar class published in the exoplanetkyoto (http://www.exoplanetkyoto.org) database without a source, however, classification is consistent with published stellar mass and effective temperature data.

‡ planet masses are reported as 1σ upper limits based on theoretical composition considerations.

The remaining superdense core candidates after mass data validation are shown below in Figure 6. Note that all of the validated masses are actually upper bounds on mass.

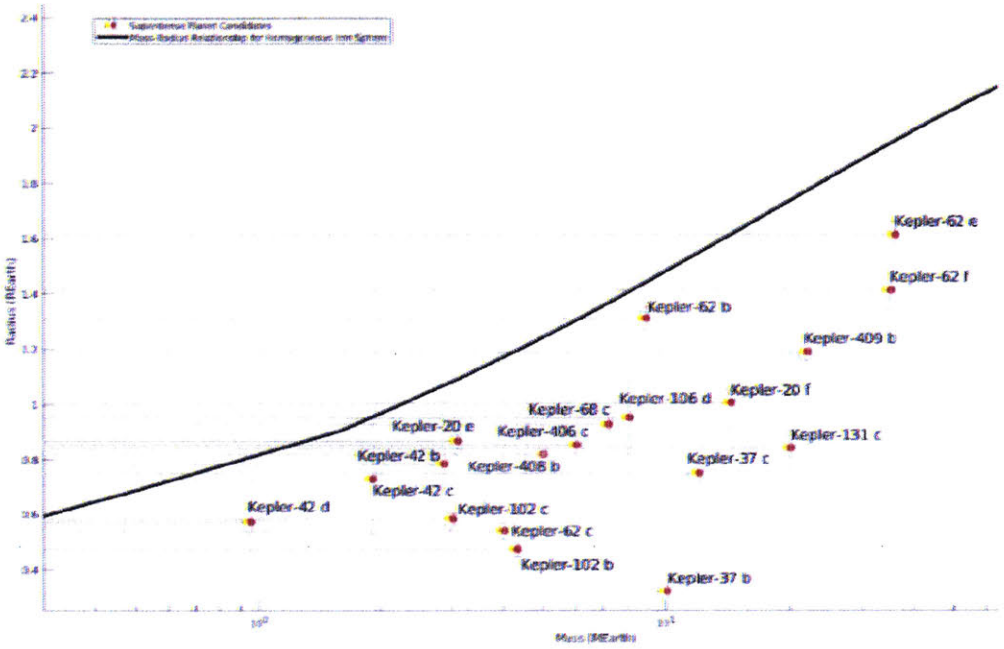

Fig 6. Updated superdense core candidates after data validation

Mass and radius (scaled by the Earth's mass and radius) for high-interest potentially superdense, mass validated candidates less than $100M_{Earth}$. The names of the planets are adjacent to their respective points. Note that all of the published mass values are upper bounds.

While the updated error on the mass measurements of the candidates shown above would have resulted in many of these them being discarded during the preliminary data gathering phase, there are now five planets (Kepler-37 b, Kepler-42 d, Kepler-62 c, Kepler-102 b, and Kepler-102 c) that appear, even with the updated uncertainties for mass, to lie nearly entirely under the iron M-R relationship, making them very likely to be anomalously dense. Even though most of the other planets identified here have uncertainty that spans the classically dense regime, for the sake of testing hypotheses, it was considered more interesting to continue to move forward without discarding them. While very few concrete conclusions can be drawn from such unconstrained data, it is still worthwhile to examine the extreme cases and understand what it may mean if they were to exist in their maximum possible density states.

4.0 ANALYSIS AND DISCUSSION

4.1 Comparison with Fossilized Core Theory

In this section, the validity of the identified 19 chthonian core candidates was checked against the assumptions of the Fossilized Core Theory. The first requirement of the theory is that the proposed cores are consistent with the core accretion model or existing estimates for the core properties of solar system gas or ice giants. The core accretion model was used as an approximation of the expected sizes of gas giant cores. While planets inconsistent with the core accretion model have been detected (Matsui *et al.*, 2007), only a rough estimate for core mass was necessary for this brief analysis. Additionally, compared to other formation mechanisms, the core accretion model has more explicit expectations for planet core masses that were convenient to use here.

The estimates for the planetary embryo properties necessary for runaway gas accretion under the core accretion model have conflicting conclusions (Mordasini *et al.*, 2008; Rice and Armitage, 2003). Some suggest that a core of 10-20M_{Earth} is required for gas giant formation (Mordasini *et al* 2008), but in simulations, others are able to show that sufficiently large (100M_{Earth}) planets are able to form under relatively short timescales (~1Myr) with a small core of only 0.6M_{Earth} (Rice and Armitage, 2003). Due to the conflicting results, for the scope of this study, analyzing the existing estimates for the measured core properties of gas and ice giants was more useful than debating the intricacies of the core accretion method, as we know that the gas giants in our solar system can and do exist with core masses as measured (albeit poorly constrained).

Uranus is thought to have an approximate core mass of 0.55M_{Earth} (Podolak *et al.*, 1995), Saturn is estimated to have a core mass of 9 - 22M_{Earth} (Saumon and Guillot, 2004; Rice and Armitage, 2003), and Jupiter is thought to have a core mass of between 12 and 45M_{Earth} (though in coming years the estimate is predicted to become more precise with new Juno data; see Guillot *et al.*, 1997; Rice and Armitage, 2003; and Saumon and Guillot, 2004). This study will be considering the upper ranges of Saturn's and Jupiter's predicted core masses, as we are interested in the extremes of possibility. Additionally, planets larger than Jupiter have been found (Luhman *et al.*, 2016), and it is not unrealistic to speculate that they might have even greater core masses than the most extreme of estimates of Jupiter's core. Figure 7 shows again the 24 superdense fossilized Chthonian core candidates as well as the estimates for the solar system's giant planet's cores.

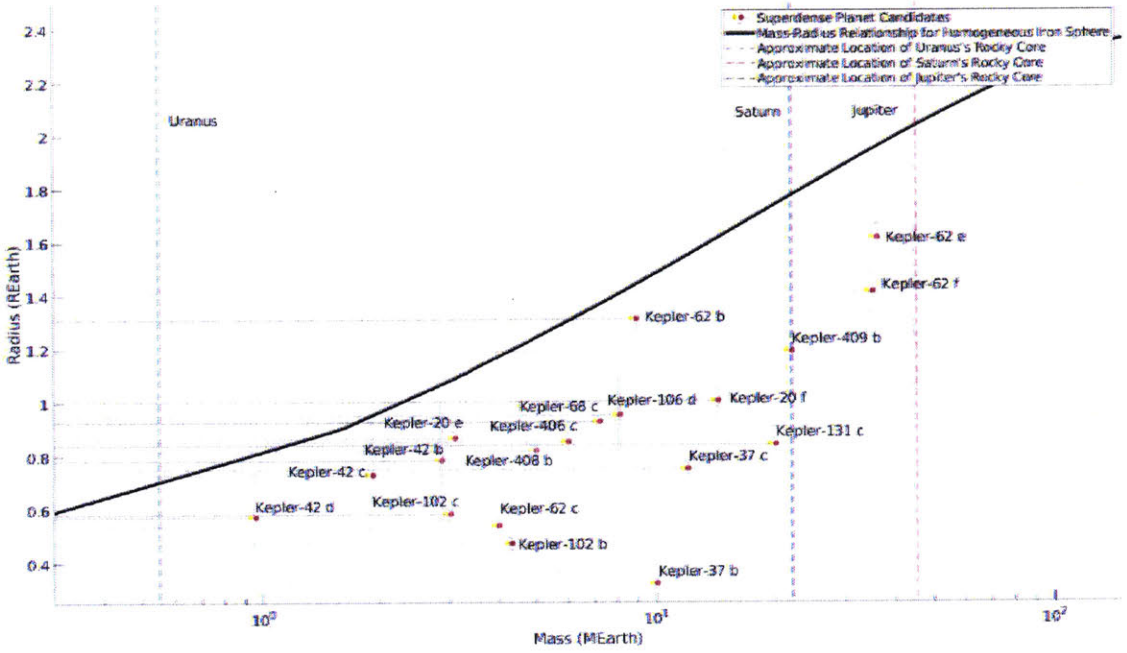

Fig. 7 A comparison of measured solar system core masses to the masses of proposed superdense fossilized cores

The black line is the mass-radius case for a homogeneous sphere of pure iron. The red points are exoplanets that have measured data implying a density greater than that of an iron sphere of the same size. The vertical dashed lines are the estimated core masses of (from right to left) Uranus, Saturn, and Jupiter. Note how all proposed candidates lie between Uranus's and Jupiter's proposed core masses.

All of the upper bound masses of the Chthonian core candidates lie within the range of known gas giant cores, supporting the theory that these planets may have previously been gas giants themselves.

The second requirement is that the semimajor axis of the core candidates is consistent with that of Hot Jupiters. In order for the required rapid hydrodynamic escape processes to occur, there needs to be significant thermal contribution from the star. The expected semimajor axis range for Hot Jupiters is less than ~0.1 - 0.2AU (though Hot Jupiters detected through the radial velocity method tend to bef biased towards semimajor axis around and greater than 0.5AU; see Currie, 2009). The Fossilized Core Theory relies on extreme conditions to explain the observed conditions, so the calculated semimajor axis data were compared to the most restrictive end of this scale at less than 0.2AU (Figure 8).

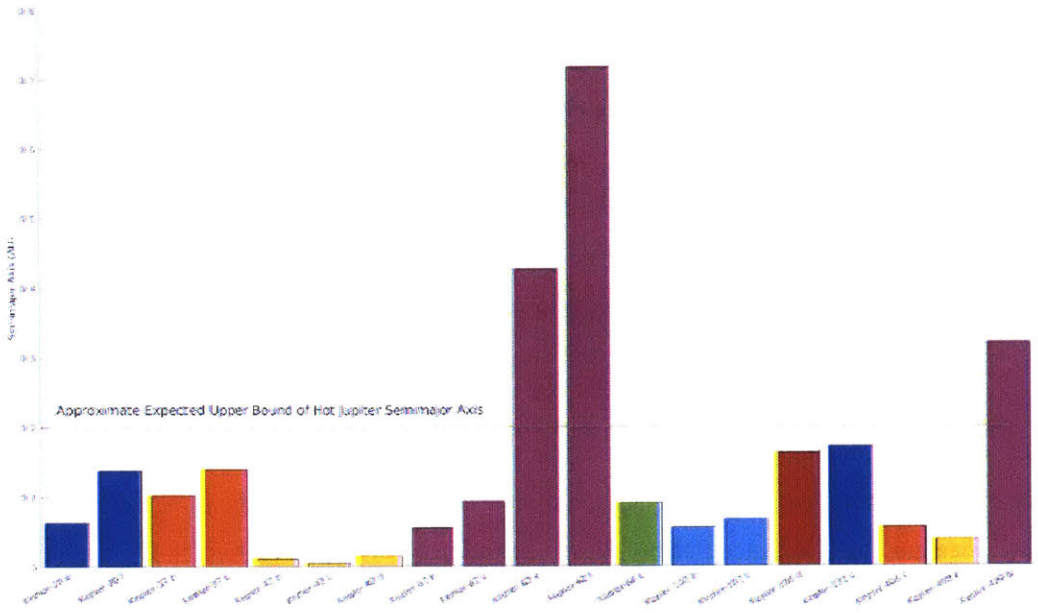

Fig. 8 Semimajor axis of superdense core candidates

Calculated semimajor axis in astronomical units of all 19 planet candidates. The green horizontal line marks a conservative upper limit for the semimajor axes of Hot Jupiters. The color of the bars corresponds to separate planetary systems, so while there are 19 planets, they represent only 11 unique planetary systems.

All but three of the Chthonian core candidate semimajor axes lie within the conservative upper bound of Hot Jupiter semimajor axes, and only one is outside of the less restrictive upper bound. Even these seemingly non-conforming cases may still be able to be explained using the Fossilized Core Theory. It is possible that they experienced several periods of migration, migrating close to their stars, losing their envelopes, and then migrating away. Alternatively, they may have experienced a hybrid loss mechanism, where their envelopes were stripped by both thermal conditions and other means, such as giant impacts.

4.2 Comparison with Giant Impact Theory

Comparison with the giant impact theory is more challenging than comparison with the fossilized core theory. The giant impact theory requires fewer specific, measurable parameters that need to be true in order for the theory to be plausible, and the assumptions made to develop explanatory models may not hold for extreme thermal and pressure cases, exotic solar system chemistry, or non-terrestrial planets.

Bonomo *et al.* (2019) relied partially on the M-R relationship of maximally collisionally stripped cores to propose Kepler-107 c as a collisional remnant, however none of planets identified here at their mass upper bounds do the same convincingly. Most of them have masses unconstrained enough that it is certainly within the realm of possibility that the planet could exist at the max collisional stripping M-R

relationship; however, this work is concerned with examining the feasibility of the density extreme. If this work looked to the entire possibility space of the mass uncertainty, the planets would be most easily explained as classically dense and perhaps rocky or volatile rich, and no more need for investigation.

But, once again, it is more interesting to move forward assuming maximum experimentally determined density regardless. The Marcus *et al.* (2010) max stripping relationship does not account for the extreme densities found here, but Marcus et al. also did not consider any compressional or extreme pressure cases when determining the prior composition of the colliding planets. The super Earth assumption also does not allow the cores to become compressed in the same way they would if they were gas giants (Mocquet *et al.*, 2014).

Inamdar and Schlichting (2016) did not explicitly investigate superdense cases, but found that in general late giant impacts of enveloped planets could increase the mean density by factors of 2 to 3. Additionally, Inamdar et al suggested that the density variation observed in the Kepler-11, Kepler-20, Kepler-36, Kepler-48, and Kepler-68 systems may be the result of such late-stage giant impacts (Inamdar and Schlichting, 2016). Two of these systems suggested to have experienced giant impacts were also identified here (Kepler-20, and Kepler-68). In general, if giant collisions could be responsible for stripping most or all of the gas envelope, a superdense compressed core could be quickly exposed while still in its compressed state, just as in the Fossilized Core Theory.

The one specific parameter that can be examined to help identify giant impact stripped chthonian candidates is through the same mechanism used by Bonomo *et al.* (2016). Kepler-107 c could be explained by the giant impact theory because it is not the innermost planet, yet it is the most dense. A similar filter was passed over the superdense planets identified in this study to see if any exist as the densest in their respective systems.

Kepler-20 e, Kepler-20 f, Kepler-68 c, Kepler-131 c, Kepler-406 c, Kepler-106 d are all superdense planets in a system with otherwise classically dense planets, and are *not* the closest planets to their stars. While this does not exclude the other planets identified here from being remnants of giant impacts, it does make these easier to analyze through this specific formation lense. It is also encouraging that both Kepler-68 and Kepler-20 appear after this filter is applied, as again these systems were identified as potentially having experienced an active colliding history by Inamdar and Schlichting (2016).

4.3 Stellar Investigation

An investigation of the spectral classes in Table 2 shows that all of the stars are main-sequence stars, and the host stars represent only four out of seven possible spectral classes. The stellar class column is slightly misleading, as most of the Chthonian core candidate planets share a solar system with another

candidate, so much of the stellar data is repeated. In order to get a better intuition for the distribution of spectral types, a histogram of spectral type (Figure 9) was plotted.

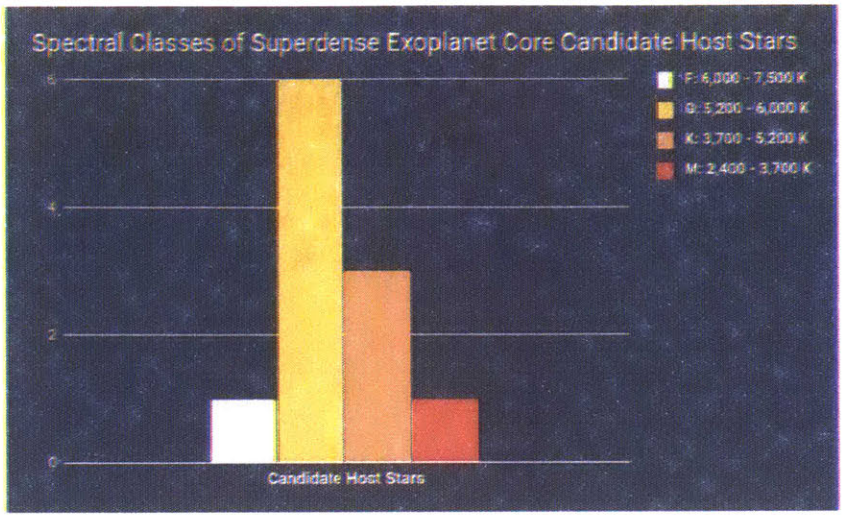

Fig. 9: Spectral classes of superdense exoplanet core candidate host stars

The solar system distribution of spectral classes for the 11 systems that contain anomalous density planets. It can be seen from this figure that over half of the host stars are *G*-type stars, and those that are not are relatively common, cool stars.

Mass, radius, and effective temperature exhibited similar clustering to the spectral classes, seen below in Table 3. The table shows the colorscaled mass, radius, and effective temperature for the superdense core candidate host stars. The colorscale highlights that, apart Kepler-42, the host stars are all very similar in mass, radius and effective temperature. Kepler-42 is an M-dwarf star, which are characteristically low-mass, small, and cool.

Table 3: Colorscaled host star mass, radius, and effective temperature

Star	Mass ($M_\odot$)	Radius ($R_\odot$)	Teff (K)
Kepler-20	0.912	0.944	5466
Kepler-37	0.803	0.77	5417
Kepler-42	0.13	0.17	3068
Kepler-62	0.69	0.63	4925
Kepler-68	1.08	1.24	5793
Kepler-102	0.81	0.74	4903
Kepler-106	1	1.04	5858
Kepler-131	1.02	1.03	5685
Kepler-406	1.07	1.07	5538
Kepler-408	1.08	1.23	6104
Kepler-409	0.92	0.89	5460

5.0 CONCLUSION

While the 19 superdense core candidates identified here have masses too poorly constrained to make definitive conclusions about their formation or evolution mechanism, some general statements can still be made about the overall patterns observed.

There are at least 19 planets that, if they exist at the upper limit of their possible mass, would be more dense than a sphere of iron of the same radius. We find five candidates (Kepler-37 b, Kepler-42 d, Kepler-62 c, Kepler-102 b, and Kepler-102 c) that after mass validation still appear to sit mostly below the iron M-R relationship, making them very likely to be anomalously dense. We investigated two potential formation and evolution mechanisms, the Fossilized Core Theory, and the Giant Impact Theory.

From the Fossilized Core Theory mechanism investigation, we find that all 19 of the plants at their mass upper bounds fall between the expected core mass of Uranus and the expected core mass of

Jupiter, making them plausibly past gas giant cores. We also find that their semimajor axes are all small (< ~0.75AU), which could potentially expose them to the thermal environments necessary to strip away their gas or ice envelopes.

From the Giant Impact Theory mechanism investigation, we find that while terrestrial planet impact scenarios cannot explain how the candidates became superdense, it is possible that gas giants undergo violent enough collisions to strip them at least partially of their gas or ice envelope. The existing models tend to focus on terrestrial planets, but previous work analyzing collisions between planets with significant envelopes can have their masses reduced in similar ways. Even without a dedicated gas giant model, similar logical steps to those used in the analysis of terrestrial planets can be applied here. As such, we identify six candidates that are not the innermost planet of their solar system, but are still anomalously dense (Kepler-20 e, Kepler-20 f, Kepler-68 c, Kepler-131 c, Kepler-406 c, Kepler-106 d).

The Fossilized Core Theory requires extreme thermal environments for the gas envelope to be lost, which implies a close proximity to the star. If there are planets that exist even closer within the same star system, it raises the question as to why the innermore planets are not also anomalously dense. Are the inner planets terrestrial planets that had no compression mechanism? Is a hybrid collisional and thermal escape scenario more likely? Without more sophisticated models and more constrained data, we cannot draw further conclusions.

We also found that while there were 19 superdense core candidates, they only represented 11 unique solar systems. This could be due to noisy data when determining planetary parameters, or it could imply a stellar component to their evolution or formation.

The investigation of the stellar properties showed that all of the host stars of the anomalously dense candidates had very typical stars. All were found to be main sequence stars, and half were found to be G-type. Additionally, the mass, radii, and effective temperatures of most of the stars closely matched our own sun. This could mean that exotic stars can exist around typical stars.

Some of these findings, however, could be the result of the Kepler mission observational schedule. Kepler used the transit method to detect exoplanets, so it was biased towards detecting planets with very short semimajor axes (Batalha *et al.*, 2010). It may not be significant that the semimajor axes of those identified here all have short periods. Similarly, Kepler's observation plan included ~60% main-sequence G-type stars. In this work, we have found that ~54% of the superdense candidates are around main-sequence G-type stars, which could just be a consequence of the demographic of stars Kepler was observing.

The most valuable next step to draw more specific conclusions would be to constrain the masses of the candidates to higher confidence levels. This would allow candidates to be accepted or denied as

superdense. Barring that, developing more sophisticated models for the relaxation rates of the compressed cores, or models of gas and ice giant envelope stripping collision events would help to understand the potential nature of the Chthonian superdense exoplanet core candidates identified here.

REFERENCES

Anglada-Escude, G., Arriagada, P., Tuomi, M., Zechmeister, M., Jenkins, J. S., Ofir, A., Dreizler, S., Gerlach, E., Marvin, C. J., Reiners, A., Jeffers, S. V., Butler, R. P., Vogt, S. S., Amado, P. J., Rodriguez-Lopez, C., Berdinas, Z. M., Morin, J., Crane, J. D., Shectman, S. A., Thompson, I. B., Diaz, M., Rivera, E., Sarmiento, L. F., Jones, H. R. A., 2014. Two planets around Kapteyn's star: a cold and a temperate super-Earth orbiting the nearest halo red dwarf. Monthly Notices of the Royal Astronomical Society: Letters. 443, 1. ppL89 - L93. https://doi.org/10.1093/mnrasl/slu076

Batalha, N. M., Borucki, W. J., Koch, D. G., Bryson, S. T., Haas, M. R., Brown, T. M., Caldwell, D. A., Hall, J. R., Gilliland, R. L., Latham, D. W., 2010. SELECTION, PRIORITIZATION, AND CHARACTERISTICS OF KEPLER TARGET STARS. The American Astronomical Society. 713, 2. https://doi.org/10.1088/2041-8205/713/2/L109

Beague, C., Nesvory, D., 2012. Multiple-planet Scattering and the Origin of Hot Jupiters. The Astrophysical Journal. 751, 2. https://doi.org/10.1088/0004-637X/751/2/119

Bonomo, A. S., Zeng, L., Damasso, M., Leinhardt, Z. M., Justeen, A. B., Lopez, E., Lund, M. N., Malavolta, L., Aguirre, V. S., Buchhave, L. A., Corsaro, E., Denman, T., Lopez-Morales, M., Mills, S. M., Mortier, A., Rice, K., Sozzetti, A., Vanderburg, A., Affer, L., Arentoft, T., Benbakoura, M., Bouchy, F., Christensen-Dalsgaard, Cameron, A. C., Cosentino, R., Dressing, C. D., Dumusque, X., Figueira, P., Fiorenzano, A. F. M., Garcia, R. A., Handberg, R., Harutyunyan, A., Johnson, J. A., Kjeldsen, H., Latham, D. W., Lovis, C., Lundkvist, M. S., Mathur, S., Mayor, M., Micela, G., Molinari, E., Motalebi, F., Nascimbeni, V., Nava, C., Pepe, F., Philips, D. F., Piotto, G., Poretti, E., Sasselov, D., Segransan, D., Udry, S., Watson, C., 2019. A giant impact as the likely origin of different twins in the Kepler-107 exoplanet system. Nature Astronomy. 3, 416-423. https://doi.org/10.1038/s41550-018-0684-9

Bouchy, F, Bonomo A. S., Santerne, A., Moutou, C., Deleuil, M., Diaz, R. F., Eggenberger, A., Ehrenreich, D., Gry, C., 2011. SOPHIE velocimetry of Kepler transit candidates III. KOI-423b: An 18 Mjup transiting companion around an F7IV star. Astronomy & Astrophysics. 533, A83. https://doi.org/10.1051/0004-6361/201117095.

Borucki, W. J., Agol, E., Fressin, F., Kaltenegger, L., Rowe, J., Isaacson, J., Fischer, D., Batalha, N., Lissauer, J. J., Marcy, G. W., Fabrycky, D., Desert, J.-M., Bryson, S. T., Barclay, T., Bastien, F., Boss, A., Brugamyer, E., Buchhave, L. A., Burke, C., Caldwell, D. A., Carter, J., Charbonneau, D., Crepp, J. R., Christensen-Dalsgaard, J., Christiansen, J. L., Ciardi, D., Chochran, W. D., DeVore, E., Doyle, L., Dupree, A. K., Endl, M., Everett, M. E., Ford, E. B. Fortney, J., Gautier, T. N., Geary, J. C., Gould, A., Haas, M., Henze, C., Howard, A. W., Howell, S. B., Huber, D., Jenkins, J. M., Kjeldsen, H., Kolbl, R., Kolodziejczak, J., Latham, D. W., Lee, B. L., Lopez, E.,

Mullally, F., Orosz, J. A., Prsa, A., Quinana, E. V., Sanchez-Ojeda, R., Sasselov, D., Seader, S., Shporer, A., Steffen, J. H., Still, M., Tenenbaum, P., Thompson, S. E., Torres, G., Twicken, J. D., Welsh, W. F., Winn, J. N., 2013. Kepler-62: A Five-Planet System with Planets of 1.4 and 1.6 Earth Radii in the Habitable Zone. Science. 340, 6132. pp 586-590. https://doi.org/10.1126/science.1234702

Brown, D., Johnson, A., Good, A.,2019. NASA's InSight Detects First Likely 'Quake' on Mars". NASA.

Catling, D., Zahnle. K., 2009. The escape of planetary atmospheres. Scientific American.

Charpinet, S., Fontaine, G., Brassard, P., Green, E. M., Grootel, V. V., Randall, S. K., Silvotti, R., Baran, A. S., Ostensen, R. H., Kawaler, S. D., Telting, J. H., 2011. A compact system of small planets around a former red-giant star. Nature. 480, 496-499. https://doi.org/10.1038/nature10631.

Chau, A/, Reinhardt, C., Helled, R., Stadel, J., 2018. Forming Mercury by Giant Impacts. The Astrophysical Journal. 865, 1. https://doi.org/10.3847/1538-4357/aad8b0

Cheng, A., Buckley, M., Steigerwald, B., 2008. Winds in Jupiter's Little Red Spot Almost Twice as Fast as Strongest Hurricane. NASA.

Croll, B., Dalba, P. A., Vanderburg, A., Eastman, J., Rappaport, S., DeVore, J., Bieryla, A., Muirhead, P. S., Han, E., Latham, D. W., Beatty, T. G., Wittenmyer, R. A., Wright, J. T., 2017. Multiwavelength Transit Observations of the Candidate Disintegrating Planetesimals Orbiting WD 1145+017. The Astrophysical Journal. 836, 82. https://doi.org/10.3847/1538-4357/836/1/82.

Currie, T., 2009. On the Semimajor Axis Distribution of Extrasolar Gas Giant Planets: Why Hot Jupiters Are Rare Around High-Mass Stars. The Astrophysical Journal Letters. 694, 2. https://doi.org/10.1088/0004-637X/694/2/L171/.

Ehrenreich, D., Jager, M., Wheatley, P. J., Lecavelier des Etangs, A., Hebrard, G., Udry, S., Bonfils, X., Delfosse, X., Desert, J. M., Sing, D. K., Vidal-Madjar, A., 2015. A giant comet-like cloud of hydrogen escaping the warm Neptune-mass exoplanet GJ 436b. Nature 422, 459-461. https://doi.org/10.1038/nature14501

Elkins-Tanton, L. T., Asphaug, E., Bell, J., Bercovici, D., Bills, B. G., Binzel, R. P., Bottke, W. F., Jun, I., Marchi, S., Oh, D., Polanskey, C. A., Weiss, B. P., Wenkert, D., Zuber, M. T., 2014. Journey to a Metal World: Concept for a Discovery Mission to Psyche (PDF). 45th Lunar and Planetary Science Conference. March 17–21, 2014. The Woodlands, Texas. No. 1777, p1253. 1253. Bibcode:2014LPI....45.1253E.

Fortney, J. J., Saumon, D., Marley, M. S., Lodders, K., Freedman, R. S., 2006. Atmosphere, Interior, and Evolution of the Metal-rich Transiting Planet HD 149026b. The Astrophysical Journal. 642, 1. https://doi.org/10.1086/500920

Frasca, A., Molenda-Zakowicz, J., De Cat, P., Catanzaro, G., Fu, J. N., Ren, A. B., Luo, A. L., Shi, J. R., Wu, Y., Zhang, H. T., 2016. Activity indicators and stellar parameters of the Kepler targets. Astronomy and Astrophysics. 594, A39. https://doi.org/10.1051/0004-6361/201628337

Fressin, F., Torres, G., Rowe, J. F., Charbonneau, D., Rogers, L. A., Ballard, S., Batalha, N. M., Borucki, W. J., Bryson, S. T., Buchhave, L. A., Ciardi, D. R., Desert, J.-M., Dressing, C. D., Fabrycky, D. C., Ford, E. B., Gautier, T. N., Henze, C. E., Holman, M. J., Howard, A., Howell, S. B., Jenkins, J. M., Koch, D. G., Latham, D. W., Lissauer, J. J., Marcy, G. W., Quinn, S. N., Ragozzine, D., Sasselov, D. D., Seager, S., Barclay, T., Mullally, F., Seader, S. E., Still, M., Twicken, J. D., Thompson, S. E., Uddin, K., 2012. Two Earth-sized planets orbiting Kepler-20. Nature. 482, 195-198. https://doi.org/10.1038/nature10780

Grasset, O., Schneider, J., Sotin, C., 2009. A study of the accuracy of mass–radius relationships for silicate-rich and ice-rich planets up to 100 Earth masses. Astrophys, J. 693, 722–733. https://doi.org/10.1086/0004-637X/693/1/722

Guenther, E. W., Barragan, O., Dai, F., Gandolfi, D., Hirano, T., Fridlund, M., Fossati, L., Chau, A., Helled, R., Korth, J., Prieto-Arrnanz, J., Nespral, D., Antoniciello, G., Deeg, H., Hjorth, M., Grziwa, S., Albrecht, S., Hatzes, A. P., Rauer, H., Csizmadia, Sz., Smith, A. M. S., Cabrera, J., Narita, N., Arriagada, P., Burt, J., Butler, R. P., Cochran, W. D., Crane, J. D., Eigmuller, Ph., Erikson, A., Johnson, J. A., Kiilerich, A., Kubyshkina, D., Palle, E., Persson, C. M., Paetzold, M., Sabotta, S., Sato, B., Shectman, St. A., Teske, J. K., Thompson, I. B., Van Eylen, V., Nowak, G., Vanderburg, A., Wittenmyer, R. A., 2017. K2-106, a system containing a metal-rich planet and a planet of lower density. Astronomy and Astrophysics, 608. https://doi.org/10.1051/0004-6361/201730885

Guillot, T., Gautier, D., Hubbard, W. B., 1997. New Constraints on the Composition of Jupiter from Galileo Measurements and Interior Models. Icarus, 30, 2. pp 534-539. https://doi.org/10.1006/icar.1997.5812

Hebrard, G., Lecavelier Des Etangs, A., Vidal-Madjar, A., Desrt, J-M., Ferlet, R., 2003. Evaporation Rate of Hot Jupiters and Formation of Chthonian Planets. Today and Tomorrow, ASP Conference Proceedings 321. arXiv:astro-ph/0312384v1

Inamdar, N. K., Schlichting, H. E., 2016. STEALING THE GAS: GIANT IMPACTS AND THE LARGE DIVERSITY IN EXOPLANET DENSITIES. The Astrophysical Journal Letters. 817, 2. https://doi.org/10.3847/2041-8205/817/2/L13

Kendall, J. D., Melosh, H. J., 2016. Differentiated Planetesimal Impacts Into a Terrestrial Magma Ocean: Fate of the Iron Core. Earth and Planetary Science Letters. 448, 24-33. https://doi.org/10.1016/j.epsl.2016.05.012

Lecavelier des Etangs, A., 2007. A diagram to determine the evaporation status of extrasolar planets. Astronomy and Astrophysics. 461, 1185-1193. https://doi.org/10.1051/0004-6361:20065014

Leger, A., Selsis, F., Sotin, C., Guillot, T., Despois, D., Mawet, D., Olliver, M., Labeque, A., Valette, C., Brachet, F., Chalzelas, B., Lammer, H., 2004. A new family of planets? 'Ocean-Planets'. Icarus. 169, 2. pp499-504. https://doi.org/10.1016/j.icarus.2004.01.001

Lissauer, J. J., Jontof-Hutter, D., Rowe, J. F., Fabrycky, D. C., Lopez, D. E., Agol, E., Marcy, G. W., Deck, K. M., Fischer, D. A., Fortney, J. J., 2013. ALL SIX PLANETS KNOWN TO ORBIT KEPLER-11 HAVE LOW DENSITIES. American Astronomical Society. 770, 2. https://doi.org/10.1088/0004-637X/770/2/131

Luhman, K. L., Esplin, T. L., Loutrel, N. P., 2016. A Census of Young Stars and Brown Dwarfs in IC 348 and NGC 1333. The Astrophysical Journal. 827, 1. https://doi.org/10.3847/0004-637X/827/1/52

Luque, R., Nowak, G., Palle, E., Dai, F., Dai, F., Kaminski, A., Nagel, E., Hidalgo, D., Bauer, F., Lafarga, M., Livingston, J., Barragan, O., Hirano, T., Fridlund, M., Gandolfi, D., Justesen, A. B., Hjorth, M., Van Eylen, V., Winn, J. N., Esposito, M., Morales, J. C., Albrecht, S., Alonso, R., Amado, P. J., Beck, P., Caballero, J. A., Cabrera, J., Cochran, W. D., Csizmadia, Sz., Deeg, H., Eigmuller, Ph., Endl, M., Erikson, A., Fukui, A., Grizwa, S., Guenther, E. W., Hatzes, A. P., Knudstrup, E., Korth, J., Lam, K. W. F., Lund, M. N., Mathur, S., Montanes-Rodriguez, P., Narita, N., Nespral, D., Niraula, P., Patzold, M., Persson, C. M., Prieto-Arranz, J., Quirrenbach, A., Rauer, H., Redfield, S., Reiners, A., Ribas, I., Smith, A. M. S., 2019. Detection and characterization of an ultra-dense sub-Neptunian planet orbiting the Sun-like star K2-292. https://doi.org/10.1051/0004-6361/201834952

Marcus, R. A., Sasselov, D, Hernquist, L., Stewart, S. T., 2010. Minimum radii of super-Earths: constraints from giant impacts. The Astrophysical Journal Letters. 712, L73-L76. https://doi.org/10.1088/2041-8205/712/1/L73

Marcy, G. W., Isaacson, H., Howard, A. W., Rowe, J. F., Jenkins, J. M., Bryson, S. T., Latham, D. W., Howell, S. B., Gautier, T. N., Batalha, N. M., Rogers, L., Ciardi, D., Fischer, D. A., Gilliland, R. L., Kjeldsen, H., Christensen-Dalsgaard, J., Huber, D., Chaplin, W. J., Basu, S., Buchhave, L. A., Quinn, S. N., Borucki, W. J., Koch, D. G., Hunter, R., Caldwell, D. A., Van Cleve, J., Kolbl, R., Weiss, L. M., Petigura, E., Seager, S., Morton, T., Johnson, J. A., Ballard, S., Burke, C., Chochram, W. D., Endl, M., MacQueen, P., Everett, M. E., Lissauer, J. J., Ford, E. B., Torres, G., Fressin, F., Brown, T. M., Steffen, J. H., Charbonneau, D., Basri, G. S., Sasselov, D. D., Winn, J., Sanchis-Ojeda, R., Christiansen, J., Adams, E., Henze, C., Dupree, A., Fabrycky, D. C., Fortney, J. J., Tarter, J., Holman, M. J., Tenenbaum, P., Shporer, A., Lucas, P. W., Welsh, W. F., Orosz, J. A., Bedding, T. R., Campante, T. L., Davies, G. R., Elsworth, Y., Handberg, R., Hekker, S., Karoff, C., Kawaler, S. D., Lund, M. N., Lundkvist, M., Metcalfe, T. S., Miglio, A., Silva Aguirre, V., Stello, D., White, T. R., Boss, A., Devore, E., Gould, A., Prsa, A., Agol, E., Barclay, T., Coughlin, J., Brugamyer, E., Mullally, F., Quintana, E. V., Still, M., Thompson, S. E., Morrison, D., Twicken, J. D., Desert, J.-M., Carter, J., Crepp, J. R., Hebrard, G., Santerne, A., Moutou, C., Sobeck, C., Hudgins, D., Haas, M. R., Robertson, P., Lillo-Box, J., Barrado, D., 2014. Masses, Radii, and Orbits of Small Kepler Planets: The Transition from Gaseous to Rocky

Planets. The Astrophysical Journal Supplement. 210, 2. https://doi.org/10.1088/0067-0049/210/2/20

Masset, F. S., Papaloizou, J. C. B., 2003. unaway Migration and the Formation of Hot Jupiters. The Astrophysical Journal. 588, 1. pp 494-508. https://doi.org/10.1086/373892.

Matsui, T., Shibai, H., Ootsubo, T., 2007. Planetary Formation Scenarios Revisited: Core-Accretion versus Disk Instability. The Astrophysical Journal. 662, 2. pp 1282-1292. https://doi.org/10.1086/517964

Mocquet, A., Grasset, O., Sotin, C., 2014. Very High-Density Planets: A Possible Remnant of Gas Giants. The Royal Society. 372. https://doi.org/10.1098/rsta.2013.0164

Molenda-Zakowich, J., Sousa, S. G., Frasca, A., Uytterhoeven, K., Briquet, M., Van Winckel, H., Drobek, D., Niemczura, E., Lampens, P., Lykke, J., Bloemen, S., Gameiro, J. F., Jean, C., Volpi, D., Gorlova, N., Mortier, A., Tsantaki, M., Raskin, G., 2013. Atmospheric parameters of 169 F-, G-, K- and M-type stars in the Kepler field. Monthly Notices of the Royal Astronomical Society. 434, 2. pp 1422-1434. https://doi.org/10.1093/mnras/stt1095

Mordasini, C., Alibert, Y., Benz, W., Naef, D., 2008. Giant Planet Formation by Core Accretion. Extreme Solar Systems. 398. p 235.

Muirhead, P. S., Johnson, J. A., Apps, K., Carter, J. A., Morton, T. D., Fabrycky, D. C., Pineda, S., Bottom, M., Rojas-Ayala, B., Schlawin, E., Hamren, K., Covey, K. R., Crepp, J. R., Stassun, K. G., Pepper, J., Hebb, L., Kirby, E. N., Howard, A. W., Isaacson, H. T., Marcy, G. W., Levitan, D., Diaz-Santos, T., Armus, L., Lloyd, J. P., 2012a. Characterizing the Cool KOIs III. KOI-961: A Small Star with Large Proper Motion and Three Small Planets. The Astrophysical Journal, 747, 2. https://doi.org/10.1088/0004-637X/747/2/144

Muirhead, P. S., Hamren, K., Schlawin, E., Rojas-Ayala, B., Covey, K. R., Lloyd, J. P., 2012b. CHARACTERIZING THE COOL KEPLER OBJECTS OF INTERESTS. NEW EFFECTIVE TEMPERATURES, METALLICITIES, MASSES, AND RADII OF LOW-MASS KEPLER PLANET-CANDIDATE HOST STARS. The Astrophysical Journal Letters. 750, 2. https://doi.org/10.1088/2041-8205/750/2/L37

Nelson, R. P., Hellary, P., Fendyke, S. M., Coleman, G., Planetary System Formation in Thermally Evolving Viscous Protoplanetary Discs. 2014. The Royal Society. 372. https://doi.org/10.1098/rsta.2013.0074

Podolak, M., Weizman, A., Marley, M., 1995. Comparative Models of Uranus and Neptune. Planetary and Space Science. 43, 12. pp 1517-1522. https://doi.org/10.1016/0032-0633(95)00061-5

Price, E. M., Rogers, L. A., 2019. Tidally-Distorted, Iron-Enhanced Exoplanets Closely Orbiting Their Stars. The Astrophysical Journal. arXiv:1901.10666

Rice, W. K. M., Armitage, P. J., 2003. On the Formation Timescale and Core Masses of Gas Giant Planets. The Astrophysical Journal Letters. 598, 1. https://doi.org/10.1086/380390

Righter, K., O'Brein, D. P., 2010. Terrestrial Planet Formation. PNAS. 108, 19165-19170. https://doi.org/10.1073/pnas.1013480108

Santerne, A., Brugger, B., Armstrong, D. J., Adibekyan, V., Lillo-Box, J., Gosselin, H., Aguichine, A., Almenara, J-M., Barrado, D., Barros, S. C. C., Bonomo, A. S., Bouchy, F., Brown, D. J. A., Deleuil, M., Delgado Mena, E., Demangeon, O., Diaz, R. F., Doyle, A., Dumusque, X., Faedi, F., Faria, J. P., Figuerira, P., Foxell, E., Giles, H., Hebrard, G., Hojjatpanah, S., Hobson, M., Jackman, J., King, G., Kirk, J., Lam, K. W. F., Ligi, R., Lovis, C., Louden, T., Mccormac, J., Mousis, O., Neal, J. J., Osborn, H. P., Pepe, F., Pollacco, D., Santos, N. C., Sousa, S. G., Udry, S., Vigan, A., 2018. An Earth-sized exoplanet with a Mercury-like composition. Nature Astronomy. 2, 5. pp 393-400. https://doi.org/10.1038/s41550-018-0420-5

Saumon, D., Guillot, T., 2004. Shock Compression of Deuterium and the Interiors of Jupiter and Saturn. The American Astronomical Society. https://doi.org/10.3847/0004-637X/819/2/127.

Seager, S., Kuchner, M., Hier-Majumder, C., Militzer, B., 2007. MASS-RADIUS RELATIONSHIPS FOR SOLID EXOPLANETS. The Astrophysical Journal. 669, 2. pp 1279-1297. https://doi.org/10.1086/521346

Sinukoff, E., Fulton, B., Scuderi, L., Gaidos, E., 2013. Below One Earth: The Detection, Formation, and Properties of Subterrestrial Worlds. Space Science Reviews. 180, 1-4, pp 71-99. https://doi.org/10.1007/s11214-013-0019-1.

Steffen, J. H., Fabrycky, D. C., Agol, E., Ford, E. B., Morehead, R. C., Cochran, W. D., Lissauer, J. J., Adams, E. R., Borucki, W. J., Caldwell, S. B. D. A., Dupree, A., Jenkins, J. M., Robertson, P., Rowe, J. F., Seader, S., Thompson, S., Twicken, J. D., 2013. Transit timing observations from Kepler – VII. Confirmation of 27 planets in 13 multiplanet systems via transit timing variations and orbital stability. 428, 2. pp 1077 - 1087. https://doi.org/10.1093/mnras/sts090.

Swift, D. C., Eggert, J. H., Hicks, D. G., Hamel, S., Casperson, K., Schwegler, E., Collins, G. W., Nettelmann, N., Ackland, G. J., 2012. Mass-Radius Relationships for Exoplanets. The American Astronomical Society. 744, 1. https://doi.org/10.1088/0004-637X/744/1/59

Tian, F., Toon, O., Pavlov, A., Sterck, H. D., 2005. Transonic Hydrodynamic Escape of Hydrogen from Extrasolar Planetary Atmospheres. The American Astronomical Society. 621, 2. https://doi.org/10.1086/427204

Tian, F., Kasting, J. F., Liu, H.-L., Roble, R. G., 2008. Hydrodynamic planetary thermosphere model: 1. Response of the Earth's thermosphere to extreme solar EUV conditions and the significance of adiabatic cooling. Journal of Geophysical Research. 113. https://doi.org/10.1029/2007JE002946

Valencia, D., O'Connell, J. O., Sasselov, D. 2006. Internal structure of massive terrestrial planets. Icarus. 181, 2. pp 545-554. https://doi.org/10.1016/j.icarus.2005.11.021

Valencia, D., Sasselov, D. D., O'Connell, R. J. O. 2007. Detailed Models of Super-Earths: How Well Can We Infer Bulk Properties?. The American Astronomical Society. 665, 2. https://doi.org/10.1086/519554

Valencia, D., Ikoma, M., Guillot, T., Nettelmann, N., 2010. Composition and Fate of Short-Period Super Earths - The Case of CoRot -7 b. Astronomy and Astrophysics. A20, 11. https://doi.org/10.1051/0004-6361/200912839

Wolf, P., Wood, E. 2007. Giant Planets: Interiors. The Outer Planets. Laboratory for Atmospheric and Space Physics.

Wu, Y., Lithwick, Y., 2011. Secular Chaos and the Formation of Hot Jupiters. The Astrophysical Journal. 735, 2. https://doi.org/10.1088/0004-637X/735/2/109

Yelle, R., Lammer, H., Ip, W.-H., 2008. Aeronomy of Extra-Solar Giant Planets. Space Science Reviews, 139, 1-4. pp 437-451. https://doi.org/10.1007/s11214-008-9420-6

Zapolsky, H.S., Salpeter, E. E., 1969. The Mass-Radius Relation for Cold Spheres of Low Mass. Astrophysical Journal, 158, p.809. https://doi.org/10.1086/150240

Zeng, L., Sasselov, D., Jacobsen, S., 2016. Mass-Radius Relation for Rocky Planets Based on PREM. The Astrophysical Journal. 819, 2. https://doi.org/10.3847/0004-637X/819/2/127.

Zeng, L., Jacobsen, S., 2017. A Simple Analytical Model for Rocky Planet Interiors. The American Astronomical Society, 837, 2. https://doi.org/10.3847/1538-4357/aa6218

ACKNOWLEDGEMENTS

Prof. Benjamin Weiss

Prof. Brent Minchew

John Brooks Biersteker

Jane Abbot

EAPS Staff

12.THU class